Molecular Cell, Vol. 11, 519–527, February, 2003, Copyright ©2003 by Cell Press

Mechanism of XIAP-Mediated Inhibition of Caspase-9

Eric N. Shiozaki,[1] Jijie Chai,[1]
Daniel J. Rigotti,[2] Stefan J. Riedl,[1]
Pingwei Li,[1] Srinivasa M. Srinivasula,[3]
Emad S. Alnemri,[3] Robert Fairman,[2]
and Yigong Shi[1,*]
[1]Department of Molecular Biology
Lewis Thomas Laboratory
Princeton University
Princeton, New Jersey 08544
[2]Department of Biology
370 Lancaster Avenue
Haverford College
Haverford, Pennsylvania 19041
[3]Kimmel Cancer Center
233 S. 10th Street
Thomas Jefferson University
Philadelphia, Pennsylvania 19107

Summary

The inhibitor of apoptosis (IAP) proteins potently inhibit the catalytic activity of caspases. While profound insight into the inhibition of the effector caspases has been gained in recent years, the mechanism of how the initiator caspase-9 is regulated by IAPs remains enigmatic. This paper reports the crystal structure of caspase-9 in an inhibitory complex with the third baculoviral IAP repeat (BIR3) of XIAP at 2.4 Å resolution. The structure reveals that the BIR3 domain forms a heterodimer with a caspase-9 monomer. Strikingly, the surface of caspase-9 that interacts with BIR3 also mediates its homodimerization. We demonstrate that monomeric caspase-9 is catalytically inactive due to the absence of a supporting sequence element that could be provided by homodimerization. Thus, XIAP sequesters caspase-9 in a monomeric state, which serves to prevent catalytic activity. These studies, in conjunction with other observations, define a unified mechanism for the activation of all caspases.

Introduction

Apoptosis is essential for the development and homeostasis of metazoans (Horvitz, 1999; Jacobson et al., 1997; Steller, 1995). Alterations in apoptotic pathways have been linked to numerous human pathologies such as cancer and neurodegenerative disorders (Thompson, 1995; Yuan and Yankner, 2000). Apoptosis is executed by cascades of caspase activation (Budihardjo et al., 1999; Shi, 2002b; Thornberry and Lazebnik, 1998). One of the well-documented cascades involves the initiator caspase, caspase-9, and the effector caspases, caspase-3 and caspase-7.

Caspases are cysteine proteases that cleave their substrates after an aspartate or glutamate residue. Cell death occurs as a result of excessive cleavage of cellular machinery by the effector caspases. However, all effector caspases are produced in cells as catalytically inactive zymogens and must be proteolytically processed to become active proteases. This activation process strictly depends on the initiator caspases, which integrate the upstream apoptotic signals and initiate the caspase activation cascades. For example, active caspase-9 cleaves and activates caspase-3 and caspase-7. Thus, the activation and inhibition of the initiator caspases constitute a central regulatory step in cellular physiology.

The inhibitor of apoptosis (IAP) family of proteins suppresses apoptosis by inhibiting the enzymatic activity of both the initiator and the effector caspases (Deveraux and Reed, 1999; Salvesen and Duckett, 2002; Shi, 2002b). At least eight members of the mammalian IAPs have been identified, including X-linked IAP (XIAP), c-IAP1, c-IAP2, and Livin/ML-IAP. Each IAP protein contains one to three copies of the 80 residue zinc binding baculoviral IAP repeat (BIR). The different BIR domains and segments in the same IAP protein appear to exhibit distinct functions. For example, the third BIR domain (BIR3) of XIAP potently inhibits the activity of the processed caspase-9 whereas the linker region between BIR1 and BIR2 selectively targets the active caspase-3 or -7 (Fesik and Shi, 2001). The IAP-mediated inhibition of all caspases can be effectively removed by the mitochondrial protein Smac/DIABLO, which is released into the cytoplasm during apoptosis (Chai et al., 2000; Du et al., 2000; Verhagen et al., 2000). The proapoptotic activity of Smac/DIABLO depends on a 4 amino acid IAP binding motif located at the N terminus of the mature protein (Liu et al., 2000; Shi, 2002a; Wu et al., 2000).

The mechanisms on the activation and inhibition of the effector caspases have been well characterized in recent years (for review see Shi, 2002b). An active effector caspase, such as caspase-7, exists as a homodimer and contains two active sites, one on each monomer. Each active site is configured by four conserved surface loops (L1, L2, L3, and L4) from one monomer and a fifth supporting loop (L2′) from the adjacent monomer. The L2′ loop, which is indispensable for the formation of an active site, cannot adopt its productive conformation until after the activation cleavage (Chai et al., 2001b; Riedl et al., 2001a). Hence, the dimeric procaspase-7 zymogen is inactive because the L2′ loop exists in an unproductive (closed) conformation. The activation cleavage allows the L2′ loop to adopt the productive (open) conformation. The active site of caspase-3 or -7 can be tightly bound by a short peptide sequence in the linker region preceding the BIR2 domain of XIAP (Chai et al., 2001a; Huang et al., 2001; Riedl et al., 2001b). This binding occludes substrate entry and catalysis, resulting in the inhibition of caspase-3 or -7.

In contrast to the effector caspases, little is known about the activation and inhibition of the initiator caspases despite intense investigation. Extensive mutagenesis studies have identified several important residues in XIAP-BIR3 that are involved in the inhibition of caspase-9 (Sun et al., 2000). In addition, a Smac-like tetrapeptide motif at the N terminus of the small subunit of

*Correspondence: yshi@molbio.princeton.edu

Table 1. Data Collection and Statistics from the Crystallographic Analysis

Beamline	CHESS-A1
Spacegroup	$P6_522$
Resolution (Å)	99.0–2.3 Å
Total observations	415,375
Unique observations	23,136
Data coverage (outer shell)	99.7% (100%)
R_{sym} (outer shell)	0.071 (0.525)
Refinement	
Resolution range (Å)	20.0–2.4 Å
Number of reflections (all)	22104
Data coverage	100%
$R_{working}/R_{free}$	0.230/0.235
Number of atoms	2806
Number of waters	215
Rmsd bond length (Å)	0.012
Rmsd bond angles (degree)	2.09
Ramachandran Plot	
Most favored (%)	84.6
Additionally allowed (%)	14.3
Generously allowed (%)	1.1
Disallowed (%)	0.0

$R_{sym} = \Sigma_h\Sigma_i|I_{h,i} - I_h|/\Sigma_h\Sigma_i\ I_{h,i}$, where I_h is the mean intensity of the i observations of symmetry related reflections of h. $R = \Sigma|F_{obs} - F_{calc}|/\Sigma F_{obs}$, where $F_{obs} = F_P$, and F_{calc} is the calculated protein structure factor from the atomic model (R_{free} was calculated with 5% of the reflections). Rmsd in bond lengths and angles are the deviations from ideal values, and the rmsd deviation in B factors is calculated between bonded atoms.

caspase-9 was found to interact with the BIR3 domain of XIAP (Srinivasula et al., 2001). Despite these advances, it was largely unclear how XIAP-mediated inhibition of caspase-9 actually occurs.

In this paper, we report the crystal structure of caspase-9 in an inhibitory complex with the BIR3 domain of XIAP, which reveals a surprising mechanism of caspase inhibition. Through binding, the XIAP-BIR3 domain traps caspase-9 in a monomeric state and deprives it of any possibility of catalytic activity. We provide several lines of additional biochemical evidence to illustrate the mechanisms of caspase-9 inhibition and regulation.

Results

Crystallization and Structure Determination

The BIR3 domain of XIAP readily forms a tight complex with caspase-9 and inhibits its catalytic activity with a potency similar to that of the intact full-length XIAP (Sun et al., 2000 and data not shown). To reveal the mechanism of XIAP-mediated inhibition of caspase-9, we sought to determine the crystal structure of a caspase-9/XIAP-BIR3 complex. After numerous trials, we were able to generate crystals of the catalytic domain of caspase-9 (residues 139–416) in an inhibitory complex with the XIAP-BIR3 domain (residues 252–350). The crystals are in the spacegroup $P6_522$ and diffract X-rays beyond 2.4 Å resolution (Table 1). The caspase-9 moiety in the asymmetric unit was located by molecular replacement using the atomic coordinates of the active half of the caspase-9 dimer as the initial search model (PDB code 1JXQ) (Renatus et al., 2001). The electron density for the bound BIR3 domain became immediately apparent after preliminary refinement. The final atomic model of the inhibitory complex has been refined to a crystallographic R factor of 23.0% (R_{free} 23.5%) at 2.4 Å resolution (Table 1).

Overall Structure of the Caspase-9/BIR3 Complex

Most strikingly, the XIAP-BIR3 domain forms a heterodimer with one caspase-9 monomer (Figures 1A and 1B). Caspases are thought to exist as homodimers (Shi, 2002b). All 18 published caspase structures, including both the initiator and the effector caspases, identify a homodimeric arrangement mediated by a predominantly hydrophobic interface (see www.rcsb.org). Recent studies indicate that, at least for caspase-3 and -7, the formation of a homodimer is a prerequisite for any catalytic activity because one of the critical supporting loops (L2′) for the active site of one monomer comes from the adjacent monomer (Chai et al., 2001b; Riedl et al., 2001a). Thus, the BIR3 domain of XIAP appears to trap caspase-9 in a monomeric state, eliminating any possibility of forming a productive active site conformation.

In the complex, the XIAP-BIR3 domain forms a large continuous interface with the caspase-9 monomer, resulting in the burial of 2200 Å^2 exposed surface area (Figures 1A and 1B). On one side of the interface, helix α5 and the linker sequence between helices α3 and α4 of BIR3 pack closely against the hydrophobic surface of caspase-9. On the other side, the N terminus of the small subunit of caspase-9 reaches out to interact with a conserved surface groove on XIAP-BIR3 (Figures 1A and 1B).

XIAP-BIR3 Traps Caspase-9 in an Inactive Conformation

Previous structural studies on the dimeric caspase-9 revealed that the active site in one monomer exists in a productive conformation while the other active site is unraveled in the adjacent monomer (Renatus et al., 2001) (Figure 1C). Interestingly, the structure of the BIR3-bound caspase-9 in the inhibitory complex is very similar to that of the inactive half of the caspase-9 dimer (Figure 1D), with a root-mean-square deviation (rmsd) of 0.97 Å for all 221 Cα atoms. In particular, the active site loops of the BIR3-bound caspase-9 closely resemble those of the inactive half of the caspase-9 dimer (Figure 1D).

To examine this scenario in detail, we compared the four active site loops from the BIR3-bound caspase-9 with those from the active half as well as the inactive half of the caspase-9 homodimer (Figure 2A). All 48 Cα atoms of the active site loops can be superimposed with an rmsd of 1.3 Å between the BIR3-bound caspase-9 and the inactive half of caspase-9. For these two cases, the L1, L2, and L3 loops exhibit nearly identical conformations whereas the L4 loops are in the same general location (Figures 2A, 2B, and 2D). In this inactive conformation, the substrate binding groove is partially occupied by the L3 loop itself. In sharp contrast, there is a large difference between the active site conformations of the BIR3-bound caspase-9 and the active half of the caspase-9 homodimer (Figures 2A, 2B, and 2C), resulting in 5.7 Å rmsd for the same 48 aligned Cα atoms. Thus, the XIAP-BIR3 domain not only sequesters caspase-9 in a monomeric state but also traps the active site loops in their unproductive conformations.

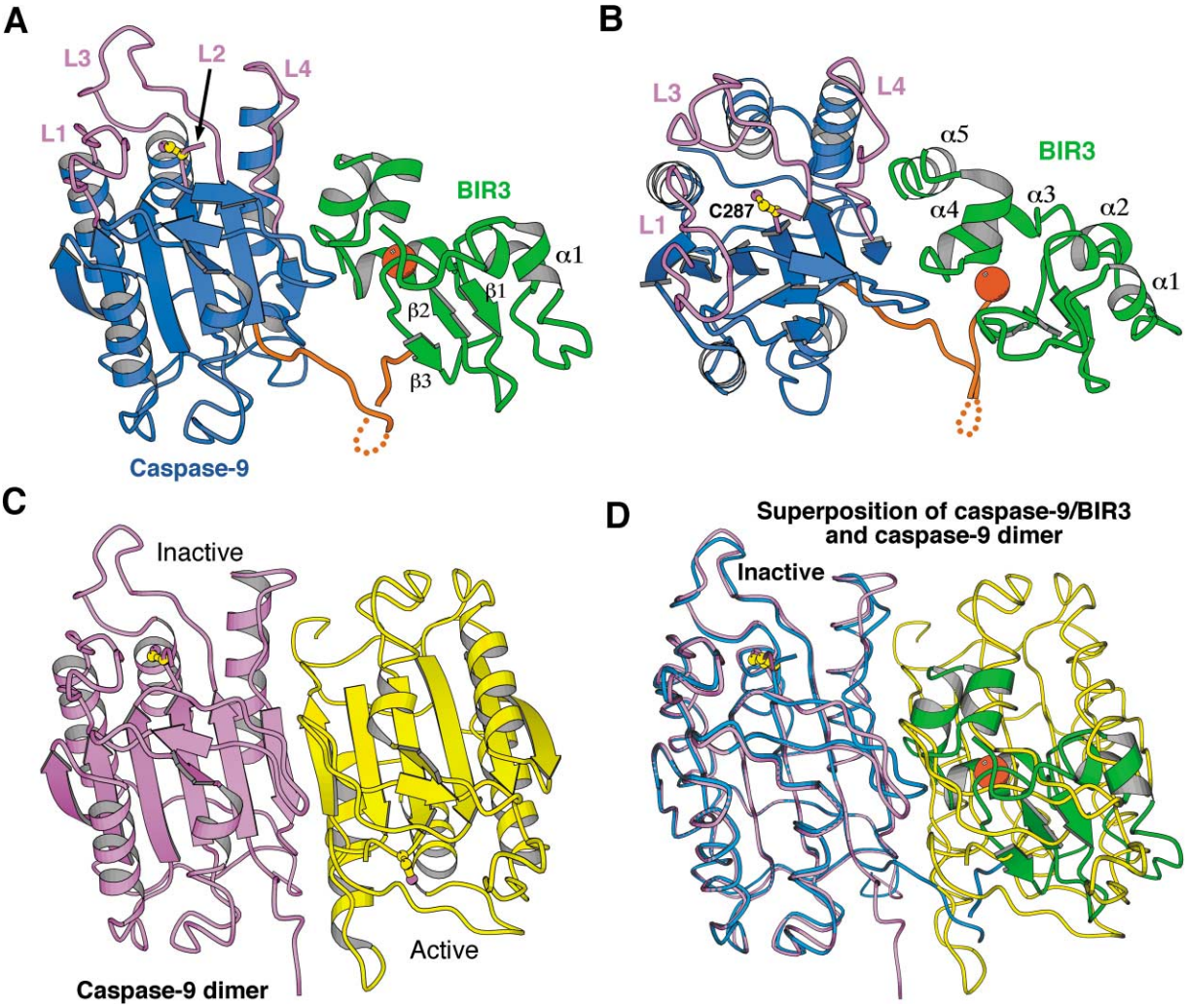

Figure 1. Crystal Structure of Caspase-9 in an Inhibitory Complex with XIAP-BIR3

(A) An overall view of the complex structure. XIAP-BIR3 binds to a large caspase-9 surface that is normally required for its homodimerization. Caspase-9 is shown in blue, with the active site loops in purple and the N terminus of the small subunit highlighted in gold. The catalytic residue, Cys287 on loop L2, is shown in ball and stick. The XIAP-BIR3 domain is colored green, with the bound zinc atom in red.

(B) A perpendicular view (relative to [A]) of the caspase-9/BIR3 complex.

(C) A schematic diagram of the published structure of the caspase-9 homodimer (Renatus et al., 2001). The active site loops of one of the two monomers (yellow) exist in an active conformation while those of the other monomer (purple) are in an inactive conformation.

(D) Superposition of the caspase-9/BIR3 complex with the caspase-9 homodimer. The coloring scheme is the same as in (A)–(C). Note that XIAP-BIR3 completely overlaps with one caspase-9 monomer. Figures 1, 2, and 3 were prepared using MOLSCRIPT (Kraulis, 1991) and GRASP (Nicholls et al., 1991).

Recognition of Caspase-9 by XIAP-BIR3

Recognition of caspase-9 by the XIAP-BIR3 domain involves a large protein-protein interface as well as a predicted interaction between the N terminus of the caspase-9 small subunit and a highly conserved surface groove on BIR3 (Srinivasula et al., 2001). This recognition is dominated by a large collection of van der Waals contacts and further supported by 11 intermolecular hydrogen bonds at the interface (Figure 3).

At the periphery of the protein-protein interface, two nonpolar residues (Pro325 and Gly326) between helices α3 and α4 of BIR3 closely stack against a hydrophobic surface formed by Leu244, Pro247, Phe404, and Phe406 of caspase-9 (Figure 3B). These interactions are supported by a specific hydrogen bond between Gln245 of caspase-9 and the backbone carbonyl group of Trp323. Interestingly, Leu244, Gln245, and Pro247 all reside in a protruding loop that is unique to caspase-9 (Earnshaw et al., 1999). This characteristic loop, with a previously undefined function, is found to play an important role in binding to the BIR3 domain of XIAP.

In the center of the protein-protein interface, Leu344 and His343 from BIR3 anchor the recognition of caspase-9 (Figure 3C). Leu344 makes multiple van der Waals interactions to a hydrophobic pocket formed by four residues (Leu384, Leu385, Ala388, and Cys403) of caspase-9. His343 accepts an intermolecular hydrogen bond from a caspase-9 backbone amide group while simultaneously making van der Waals contacts to Cys 403, Phe404, and Phe496 of caspase-9 (Figure 3C).

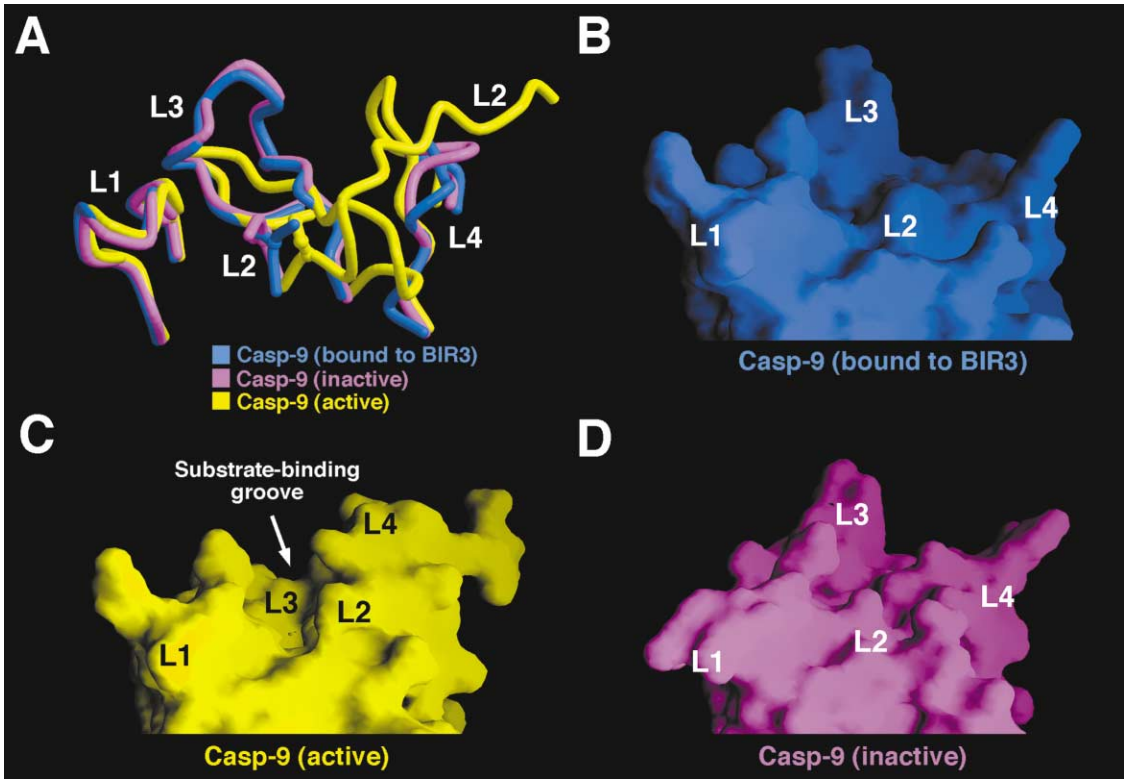

Figure 2. The Active Site of the BIR3-Bound Caspase-9 Exists in an Unproductive Conformation

(A) Superposition of the four active site loops from the BIR3-bound caspase-9 (blue) and the active (yellow) and inactive (purple) monomers of the caspase-9 homodimer. The active site conformation of the BIR3-bound caspase-9 closely resembles that of the inactive caspase-9 monomer.

(B) Surface representation of the active site loops in the BIR3-bound caspase-9.

(C) Surface representation of the active site loops in the active caspase-9 monomer. Note the presence of the substrate binding groove.

(D) Surface representation of the active site loops in the inactive caspase-9 monomer.

The N-terminal four amino acids of the caspase-9 small subunit (Ala316-Thr317-Pro318-Phe319) conform to the Smac-like IAP binding motif (Shi 2002a; Srinivasula et al., 2001). This peptide sequence by itself is sufficient for the binding to XIAP-BIR3, and mutation of this sequence abolished BIR3-mediated inhibition of caspase-9 due to the loss of binding (Srinivasula et al., 2001). This tetrapeptide was predicted to bind to the conserved surface groove of BIR3 in the same manner as the N terminus of the mature Smac protein (Srinivasula et al., 2001). Indeed, this interaction is just as predicted, with Ala316 playing the anchoring role in this part of the interface (Figure 3D). Interestingly, this IAP binding motif does not just bind to the BIR3 domain in isolation; it also packs against two adjacent caspase-9 residues, Pro336 and Pro338, through van der Waals contacts (Figure 3D). These interactions mold the caspase-9 peptide-BIR3 binding into the larger and continuous protein-protein recognition interface (Figure 3A).

Pro336 and its adjacent residues of caspase-9 constitute the core element of the L2′ loop in stabilizing the productive conformation of the active site loops in the structure of the caspase-9 homodimer (Renatus et al., 2001). However, in the inhibitory caspase-9/BIR3 complex, this region is involved in stabilizing the interactions between the IAP binding motif of caspase-9 and the BIR3 domain. This analysis further reinforces the notion that XIAP-BIR3 not just sequesters caspase-9 in its monomeric form but also traps the active site loops in their unproductive conformations.

Mutational Analysis

To corroborate our structural observation, we devised a caspase-9 assay using its physiological substrate, procaspase-3 zymogen, and investigated the ability of various XIAP-BIR3 point mutants to inhibit caspase-9. A mutation on the catalytic residue, Cys163 to Ala, was introduced in the substrate procaspase-3 to prevent its self-activation or cleavage. As anticipated, the wild-type (WT) caspase-9 cleaved the procaspase-3 precursor into p17 and p12 fragments (Figure 3E, lane 1), and incubation with the WT BIR3 protein (residues 252–350) resulted in the efficient inhibition of this activity (lane 2). In contrast to the WT protein, mutation of any of the four critical residues of BIR3 (P325G, G326E, H343A, and L344A) led to loss of this inhibition as judged by the cleavage of procaspase-3 precursor (Figure 3E, lanes 4, 5, 8, and 9). The result that H343A can no longer inhibit caspase-9 confirms an earlier report (Sun et al., 2000). These residues make important contributions to the recognition and sequestration of the caspase-9 monomer (Figures 3B–3D); mutation of any of these residues presumably destabilizes the interface, allowing the formation of the caspase-9 homodimer and subsequent restoration of catalytic activity. It is of particular note that none of these mutations affects the conserved surface

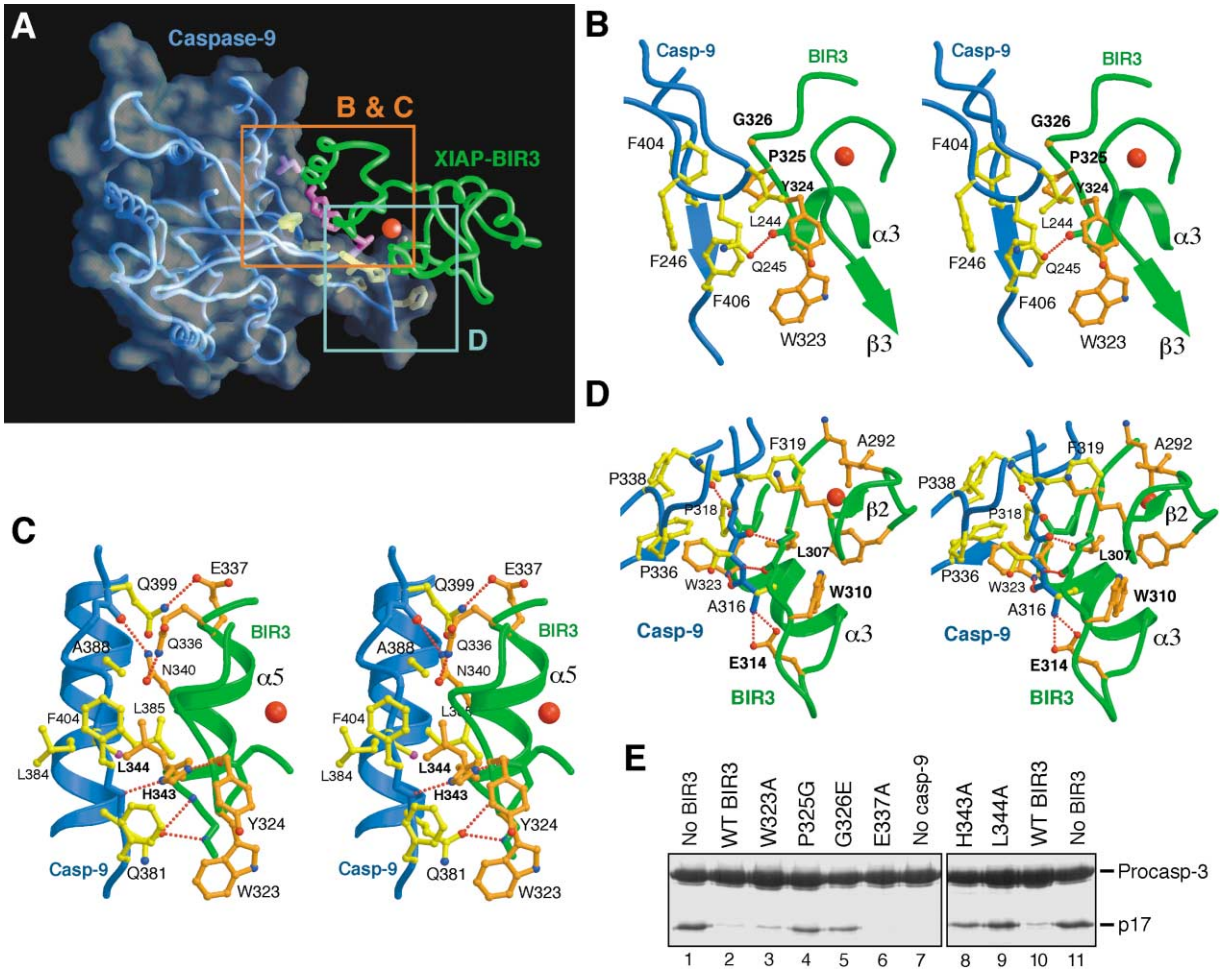

Figure 3. Recognition of Caspase-9 by the BIR3 Domain of XIAP

(A) An overall view on the structure of the complex. Caspase-9 and BIR3 are shown as blue and green coil, respectively. A number of critical interface residues from caspase-9 and BIR3 are colored yellow and purple, respectively. To illustrate the complementary binding, the transparent surface contour of caspase-9 is shown.

(B) A stereo view on the interface centered around Pro325 and Gly326 of XIAP. The overall coloring scheme is the same as in Figure 1. The side chains from key residues in caspase-9 and XIAP-BIR3 are colored yellow and gold, respectively. Hydrogen bonds are represented by red dashed lines.

(C) A stereo view on the interface centered around His343 and Leu344 of XIAP. The side chain of His343 makes two hydrogen bonds to bridge caspase-9 and BIR3 whereas Leu344 packs against multiple hydrophobic residues in caspase-9.

(D) A stereo depiction on the recognition of BIR3 by the N-terminal IAP binding motif of caspase-9. The tetrapeptide motif (Ala316-Thr317-Pro318-Phe319) binds to the conserved surface of BIR3 as predicted (Srinivasula et al., 2001). This binding is augmented by the close packing interactions from Pro336 and Pro338 of caspase-9.

(E) Functional consequence of point mutations on critical residues of XIAP-BIR3. Cleavage of the procaspase-3 substrate by caspase-9 was performed in the absence or presence of various XIAP-BIR3 point mutants. The results were visualized by SDS-PAGE followed by Coomassie blue staining. The generation and purification of caspase-9 and XIAP-BIR3 mutant proteins and the caspase-9 assay are described in the Experimental Procedures. The procaspase-3 (C163A) precursor was used as the substrate.

groove on BIR3; thus, caspase-9 is still able to bind to the mutated BIR3 domain but is no longer subject to its inhibition (Sun et al., 2000 and data not shown).

These observations also confirm the important concept that recognition of caspase-9 by IAPs is necessary but not sufficient for its inhibition. Although the mutant XIAP-BIR3 forms a stable complex with caspase-9, it cannot efficiently inhibit caspase-9 because it fails to prevent caspase-9 homodimerization through the other important protein-protein interface. Similarly, the BIR3 domain from either c-IAP1 or c-IAP2 can bind to the IAP binding motif of caspase-9 (data not shown); yet neither c-IAP1 nor c-IAP2 is expected to inhibit caspase-9. The reasons are clear: Gly326 of XIAP is replaced by a charged and bulky residue Arg in c-IAP1 and c-IAP2. In addition, His343 and Leu344 of XIAP are replaced by Gln-Gly and Gln-Ala in c-IAP1 and c-IAP2, respectively. These changes are expected to disrupt the packing interactions of the protein-protein interface between caspase-9 and BIR3 and hence are unable to prevent the homodimerization of caspase-9.

Monomeric Caspase-9 Is Catalytically Inactive Due to Loss of the L2′ Loop

Our previous studies on effector caspases demonstrate that a productive conformation of the active site on one

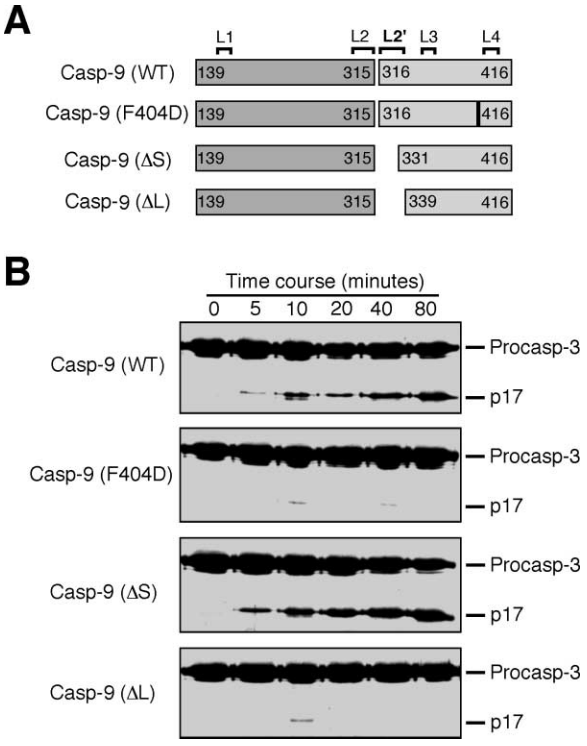

Figure 4. Monomeric Caspase-9 Is Inactive Due to the Lack of the Critical L2′ Loop

(A) A schematic diagram of four caspase-9 variants. Using a coexpression strategy, these proteins were produced in their cleaved form (see Experimental Procedures for details). The approximate positions of the five essential loops in caspase-9 are indicated.

(B) A time course of procaspase-3 cleavage by the four caspase-9 variants. p17 represents the cleaved product. Assays were performed as described in the Experimental Procedures.

monomer must involve the participation of the critical L2′ loop on the adjacent monomer, which forms a loop bundle with the L2 and L4 loops through specific interactions (Chai et al., 2001b; Riedl et al., 2001a). This result indicates that an effector caspase must be in its dimeric form to exhibit any catalytic activity. Since the conformations of the active site loops are highly conserved among the effector and the initiator caspases (Shi, 2002b), the L2′ loop is likely to be essential for the initiator caspases as well. This hypothesis predicts that monomeric caspase-9 must be catalytically inactive.

To examine this hypothesis, we generated a monomeric caspase-9 by mutating Phe404, which resides in the center of the homodimerization interface, to a negatively charged residue Asp (Figure 4A). This mutation is expected to eliminate homodimerization of caspase-9 as burying two charged residues in the center of a predominantly hydrophobic interface is energetically extremely unfavorable. Indeed, this mutant caspase-9 (F404D) exists exclusively as a monomer in solution (data not shown and see below). As anticipated, caspase-9 (F404D) did not exhibit any detectable enzymatic activity (Figure 4B), despite the presence of all sequence elements required to form an active site.

Next, we examined whether the L2′ loop in caspase-9 plays the same essential role as in caspase-3 and -7. Using a coexpression strategy, we generated three caspase-9 variants (Figure 4A), each of which contains an invariant large subunit (residues 139–315) and a distinct small subunit. Thus, these caspase-9 variants represent their "cleaved" or "active" form. The only difference is that, relative to the WT caspase-9, the ΔS and ΔL variants contain deletion of residues 316–330 and 316–338, respectively (Figure 4A). Removal of the fragment 316–330 does not affect any residue implicated in the stabilization of the active site conformation and hence should not have any negative impact on the catalytic activity of caspase-9. However, since the removal of residues 331–338 eliminates the formation of the loop-bundle, caspase-9 (ΔL) was expected to be inactive.

In our in vitro caspase-9 assays, equal amounts of the caspase-9 variants were incubated with the procaspase-3 (C163A) substrate; the cleavage efficiency was monitored by SDS-PAGE and Coomassie staining (Figure 4B). In complete agreement with our structure-based prediction, caspase-9 (ΔL) did not exhibit a detectable level of catalytic activity compared to the WT protein. In contrast, caspase-9 (ΔS) was approximately 2-fold more active than the WT protein (Figure 4B). This is likely due to the elimination of the 15 flexible residues (315–330), which may impede substrate entry into the active site during catalysis.

Our data demonstrate that the L2′ loop plays an indispensable role in stabilizing the conformation of the four active site loops (L1–L4) of caspase-9. This is the primary reason why a monomeric caspase-9 is inactive in solution. To further confirm this conclusion, we mutated Asp293 to Ala in caspase-9. Asp293, conserved among several caspases (Chai et al., 2001b), is located on loop L2 and makes critical contacts to residues on the L2′ loop. Thus, this mutation is expected to disrupt the formation of the loop bundle involving loops L2′ and L4. Indeed, caspase-9 (D293A) exhibited an undetectable level of activity compared to the WT enzyme (data not shown).

Caspase-9 Exists Mostly as a Monomer in Solution

An earlier report suggested that caspase-9 exists in an equilibrium between a large population of monomers and a small population of homodimers as judged by gel filtration (Renatus et al., 2001). The dimeric form of caspase-9 was found to be active whereas the monomeric form was largely inactive (Renatus et al., 2001). In all our attempts, we have consistently observed a single species of caspase-9 in solution by gel filtration as well as by a variety of other criteria.

To accurately determine the basal state of caspase-9 in solution, we examined the molecular weight of caspase-9 by sedimentation equilibrium analysis using analytical ultracentrifugation (Table 2). Little, if any, variation in molecular weight as a function of rotor speed was observed for any of the caspase-9 samples, indicating that the protein behaves mostly as a single species in solution (data not shown). Interestingly, both the processed caspase-9 and the unprocessed procaspase-9 zymogen were found to have a molecular weight consistent with that of a monomer. In addition, this analysis confirms that the XIAP-BIR3 domain forms a stable heterodimer with the caspase-9 monomer (Table 2). In contrast, we demonstrate that the active caspase-7, which

Table 2. A Summary of the Analytical Ultracentrifugation Measurements

Sample	Concentration	Molecular Weight (Dalton)	
		Observed	Calculated
Caspase-9 (active)			
	20 μM	28,500 ± 700	31,297
	10 μM	31,120 ± 1540	31,297
Caspase-9/XIAP-BIR3			
	20 μM	39,380 ± 1220	42,973
	10 μM	41,060 ± 1530	42,973
	5 μM	42,200 ± 2440	42,973
Caspase-7			
	20 μM	54,530 ± 1070	29,865
	10 μM	49,720 ± 2440	29,865
Procaspase-9 zymogen			
	20 μM	29,920 ± 1400	31,457
	10 μM	27,840 ± 2150	31,457

Molecular weight represents global analysis of data collected at four rotor speeds, 10 K, 15 K, 20 K, and 25 K rpm. All data were collected at 4°C. The caspase-9/XIAP-BIR3 sample contains the wild-type caspase-9 residues 139–315 and 316–416 and XIAP residues 252–350. The active caspase-9 contains residues 139–315 and 316–416, except that residues Glu304-Asp305-Glu306 have been replaced by three Ala residues to reduce limited proteolysis by the intrinsic enzymatic activity of caspase-9. The procaspase-9 zymogen contains residues 139–416. The active caspase-7 contains residues 51–198 and 200–303.

is known to be dimeric, indeed exhibits a molecular weight consistent with that of a dimer (Table 2).

If the processed caspase-9 is mostly a monomer in solution, how can it exhibit any catalytic activity in isolation? As shown by a published report (Renatus et al., 2001) and our own results (Figure 4 and Chai et al., 2001b), this activity is clearly due to the transient formation of caspase-9 homodimers.

Discussion

A mechanistic paradigm on the regulation of caspase-9 activation and inhibition has emerged from this study (Figure 5). At the basal state, both the procaspase-9 zymogen and the processed caspase-9 exist mostly as a monomer. These monomers have the potential to be activated (by Apaf-1, for example) or inhibited (Figure 5). XIAP potently inhibits the catalytic activity of caspase-9 by using the BIR3 domain to heterodimerize with a caspase-9 monomer through the same interface that is required for the homodimerization of caspase-9 (Figure 5). Thus, XIAP traps caspase-9 in an inactive monomeric state, preventing any possibility of its homodimerization (Figure 5). Furthermore, the four active site loops in the BIR3-bound caspase-9 exist in an unproductive conformation, and the fifth loop, loop L2′, is directly involved in the interaction between XIAP and caspase-9 (Figure 3D). Thus, the caspase-9/BIR3 structure also shows, in a broad sense, how a protein inhibitor can mess up the active state of a protease by trapping half of it (the monomer) in an inactive state. This mechanism prevents the assembly of a functional protease.

Caspase-9, one of the best-characterized initiator caspases, plays an important role in apoptosis and directly activates the effector caspases-3 and -7. Although XIAP potently inhibits the catalytic activity of both caspase-9 and caspase-3/-7, the underlining mechanisms are entirely different. In the case of the effector cas-

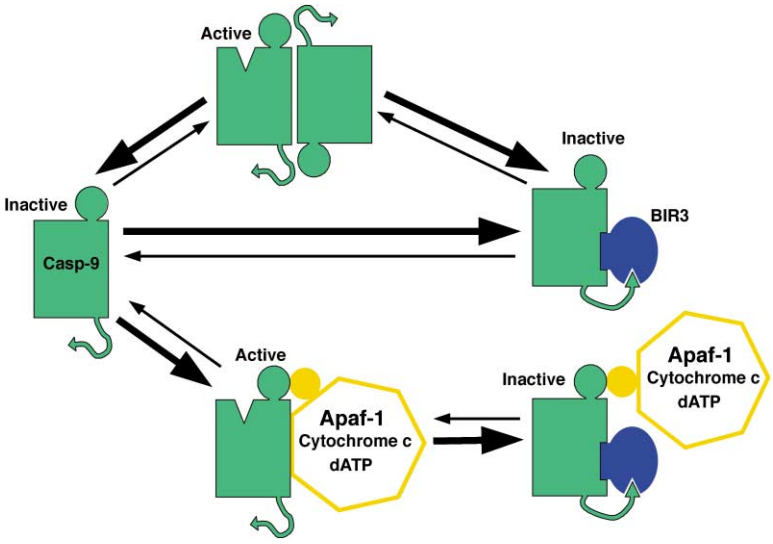

Figure 5. A Schematic Diagram of Caspase-9 Activation and Inhibition

The full-length caspase-9 is colored green, with the prodomain (CARD) shown as a circle. The thickness of the black arrows indicates the preference of the equilibrium. Caspase-9 can be activated by the apoptosome comprising Apaf-1, cytochrome c, and the critical cofactor dATP/ATP. Both isolated caspase-9 and the apoptosome-activated caspase-9 are subject to XIAP-mediated inhibition. See text for a detailed discussion.

pases, the active site is occupied by a small peptide sequence immediately preceding the BIR2 domain of XIAP (Chai et al., 2001a; Huang et al., 2001; Riedl et al., 2001b). Although unique in its own features, this mechanism falls into the frequently observed theme in the protease/inhibitor paradigm of inhibition by blocking the active site. For caspase-9, however, only the inactive monomer is trapped by the BIR3 domain of XIAP through an extensive protein-protein interface. Thus, complete inhibition of enzymatic activity by XIAP is achieved without even touching the active site of caspase-9.

The recognition interface between caspase-9 and XIAP-BIR3 has two components. The binding between the IAP binding tetrapeptide of caspase-9 and the conserved surface groove on XIAP-BIR3 is necessary but not sufficient for any XIAP-mediated inhibition. An additional protein-protein interface must be present to direct the inhibition specificity. This conclusion allows us to explain many published observations. For example, despite the removal of a 15 residue peptide containing the Smac-like IAP binding motif in the small subunit, the enzymatic activity of the resulting caspase-9 can still be inhibited by XIAP (Zou et al., 2002). In this case, although the N terminus of the small subunit (AISS) alone is unable to form a stable complex with the BIR3 domain of XIAP, it can do so in the context of the caspase-9 protein because the other significant protein-protein interface cooperates with this weak peptide-BIR3 binding to yield a stable complex.

Caspases were mainly regarded as constitutive homodimers. This concept was derived from well over a dozen crystal structures, which showed again and again that both the initiator and the effector caspases are homodimers (Shi, 2002b). However, careful evaluation of all previous data really only reveals that the active caspases are homodimers. The reason why a caspase by itself must homodimerize in order to have any catalytic activity lies in the fact that the active site of a caspase monomer needs the critical support of an additional sequence element, the L2′ loop, which cannot be provided by the caspase monomer itself (Shi, 2002b). Thus, dimerization can drive the activation of the initiator caspase, caspase-9, a concept initially proposed by Guy Salvesen and colleagues (Renatus et al., 2001). This concept is further supported by our report that both the processed caspase-9 and the procaspase-9 zymogen exist mostly as a monomer in solution (Table 2). We arrived at this conclusion using analytical ultracentrifugation analysis, which represents the ideal method for the determination of molecular weights for macromolecular assemblies.

Although our studies pinpoint the mechanisms of XIAP-mediated inhibition of caspase-9 and shed considerable light on its activation process, we cannot yet explain how Apaf-1 activates caspase-9 in the presence of cytochrome c and dATP (Li et al., 1997; Shi, 2001). It is of particular note that, although dimerization of caspase-9 is needed for its activity, when tested on its own in vitro, the mechanism of Apaf-1-mediated activation of caspase-9 may have nothing to do with the dimerization process. The reason is that dimerization merely provides the L2′ loop for the active site of one monomer. If the apoptosome can somehow substitute for the badly needed L2′ loop for the caspase-9 monomer, it can certainly be activated without homodimerization (Figure 5). More importantly, it is unclear whether the catalytic activity of a caspase-9 homodimer is identical or similar to that of the apoptosome-activated caspase-9. If this turns out to be true, then what the apoptosome does could be to promote the dimerization of caspase-9. In this case, the puzzling question would be why the apoptosome has a 7-fold symmetry. It should be noted that, even in this case, it remains possible that the apoptosome activates caspase-9 using a different mechanism compared to the homodimerization of caspase-9, yet the end result is the same. On the other hand, if the catalytic activity of the homodimerized caspase-9 is significantly less than that of the apoptosome-activated caspase-9, then the concept of "dimerization drives the activation of initiator caspases" certainly needs to be reevaluated. In any case, a definitive answer on this issue awaits a detailed structural analysis.

Experimental Procedures

Protein Preparation

All constructs were generated using a standard PCR-based cloning strategy, and the identities of individual clones were verified through double-stranded plasmid sequencing. To minimize self-cleavage in bacteria, the catalytic subunit of caspase-9 (residues 139–416, in vector pET-21b) was coexpressed with the BIR3 domain of XIAP (residues 252–350, in vector pBB75) in *Escherichia coli* strain BL21(DE3). A serendipitous bonus from this coexpression is a large quantity of unprocessed procaspase-9 zymogen. The soluble fraction of the caspase-9/BIR3 complex and the procaspase-9 zymogen in the *E. coli* lysate were purified using a Ni-NTA (Qiagen) column and further fractionated by anion-exchange (Source-15Q, Pharmacia) and gel-filtration chromatography (Superdex-200, Pharmacia). Recombinant active caspase-7 and missense mutants of caspase-9 and XIAP-BIR3 were overexpressed and purified as described (Chai et al., 2001a, 2001b). For the three caspase-9 deletion variants (Figure 4A), the large and the small subunits were coexpressed and purified as described (Chai et al., 2001b).

Crystallization and Data Collection

Crystals of the caspase-9/BIR3 complex were grown by the hanging-drop vapor-diffusion method by mixing protein with an equal volume of reservoir solution. The well buffer contains 100 mM Tris (pH 8.0), 1.0 M potassium monohydrogen phosphate, and 0.2 M sodium chloride. Small crystals appeared after 3 weeks, with a typical size of $0.1 \times 0.1 \times 0.3$ mm^3. The crystals belong to the space group $P6_522$, contain one complex in each asymmetric unit, and have a unit cell dimension of $a = b = 104.42$ Å and $c = 170.31$ Å. Crystals were equilibrated in a cryoprotectant buffer containing well buffer plus 24% glycerol and were flash frozen in a -170°C nitrogen stream. The native data were collected at the CHESS beamline A1. The data were processed using the software Denzo and Scalepack (Otwinowski and Minor, 1997).

Structure Determination and Refinement

The structure was determined by Molecular Replacement, using the software AMoRe (Navaza, 1994). The atomic coordinates of the active half of the caspase-9 dimer (PDB code 1JXQ) were used for rotational and subsequent translational searches against a 15–3.0 Å data set, which yielded a single promising solution with high correlation factors. The candidate solution was checked in the program O (Jones et al., 1991) and subjected to rigid body refinement using CNS (Terwilliger and Berendzen, 1996). The electron density for the BIR3 domain was unambiguous. The BIR3 moiety was built in, and the caspase-9/BIR3 complex was refined further by simulated annealing using CNS. The final refined atomic model ($R_{free} \sim 0.235$) contains residues 256–346 for XIAP-BIR3, residues 140–288, 316–320, and 333–416 for caspase-9, 215 ordered water molecules, and one zinc atom at 2.4 Å resolution.

Caspase-9 Assay

The reaction was performed at 37°C under the following buffer conditions: 25 mM HEPES (pH 7.5), 100 mM KCl, and 1 mM dithiothreitol (DTT). The substrate (procaspase-3, C163A) concentration was approximately 80 μM. Caspase-9 variants were diluted to the same concentration (0.3 μM) with the assay buffer. Reactions were stopped with the addition of equi-volume 2× SDS loading buffer and boiled for three minutes. The samples were applied to SDS-PAGE, and the results were visualized by Coomassie staining.

Analytical Ultracentrifugation

Protein samples were prepared in 10 mM Tris-HCl (pH 8.0), 100 mM NaCl, and 2 mm DTT. All sedimentation equilibrium experiments were carried out at 4°C using a Beckman Optima XL-A analytical ultracentrifuge equipped with an An60 Ti rotor and using six-channel, 12 mm path length, charcoal-filled Epon centerpieces, and quartz windows. Data were collected at four rotor speeds (10,000, 15,000, 20,000, and 25,000 rpm) and represent the average of 20 scans using a scan step-size of 0.001 cm. Partial specific volumes and solution density were calculated using the Sednterp program. Data were analyzed using the WinNONOLIN program from the Analytical Ultracentrifugation Facility at the University of Connecticut (Storrs, CT).

Acknowledgments

We thank Lana Welch at CHESS for help and Noel Hunt for administrative assistance. E.N.S. thanks R.M. Tanner for her consistent encouragement and assistance. This research was supported by NIH grants CA90269 (to Y.S.) and AG14357 (to E.S.A.), and a predoctoral fellowship from the New Jersey Commission on Cancer Research (E.N.S.). S.M.S. is a special fellow of the Leukemia and Lymphoma Society.

Received: December 27, 2002
Revised: January 16, 2003

References

Budihardjo, I., Oliver, H., Lutter, M., Luo, X., and Wang, X. (1999). Biochemical pathways of caspase activation during apoptosis. Annu. Rev. Cell Dev. Biol. *15*, 269–290.

Chai, J., Du, C., Wu, J.-W., Kyin, S., Wang, X., and Shi, Y. (2000). Structural and biochemical basis of apoptotic activation by Smac/DIABLO. Nature *406*, 855–862.

Chai, J., Shiozaki, E., Srinivasula, S.M., Wu, Q., Datta, P., Alnemri, E.S., and Shi, Y. (2001a). Structural basis of caspase-7 inhibiton by XIAP. Cell *104*, 769–780.

Chai, J., Wu, Q., Shiozaki, E., Srinivasula, S.M., Alnemri, E.S., and Shi, Y. (2001b). Crystal structure of a procaspase-7 zymogen: mechanisms of activation and substrate binding. Cell *107*, 399–407.

Deveraux, Q.L., and Reed, J.C. (1999). IAP family proteins—suppressors of apoptosis. Genes Dev. *13*, 239–252.

Du, C., Fang, M., Li, Y., and Wang, X. (2000). Smac, a mitochondrial protein that promotes cytochrome c-dependent caspase activation during apoptosis. Cell *102*, 33–42.

Earnshaw, W.C., Martins, L.M., and Kaufmann, S.H. (1999). Mammalian caspases: structure, activation, substrates, and functions during apoptosis. Annu. Rev. Biochem. *68*, 383–424.

Fesik, S.W., and Shi, Y. (2001). Controlling caspases. Science *294*, 1477–1478.

Horvitz, H.R. (1999). Genetic control of programmed cell death in the nematode Caenorhabditis elegans. Cancer Res. *59*, 1701–1706.

Huang, Y., Park, Y.C., Rich, R.L., Segal, D., Myszka, D.G., and Wu, H. (2001). Structural basis of caspase inhibition by XIAP: differential roles of the linker versus the BIR domain. Cell *104*, 781–790.

Jacobson, M.D., Weil, M., and Raff, M.C. (1997). Programmed cell death in animal development. Cell *88*, 347–354.

Jones, T.A., Zou, J.-Y., Cowan, S.W., and Kjeldgaard, M. (1991). Improved methods for building protein models in electron density maps and the location of errors in these models. Acta Crystallogr. A *47*, 110–119.

Kraulis, P.J. (1991). Molscript: a program to produce both detailed and schematic plots of protein structures. J. Appl. Crystallogr. *24*, 946–950.

Li, P., Nijhawan, D., Budihardjo, I., Srinivasula, S.M., Ahmad, M., Alnemri, E.S., and Wang, X. (1997). Cytochrome c and dATP-dependent formation of Apaf-1/caspase-9 complex initiates an apoptotic protease cascade. Cell *91*, 479–489.

Liu, Z., Sun, C., Olejniczak, E.T., Meadows, R.P., Betz, S.F., Oost, T., Herrmann, J., Wu, J.C., and Fesik, S.W. (2000). Structural basis for binding of Smac/DIABLO to the XIAP BIR3 domain. Nature *408*, 1004–1008.

Navaza, J. (1994). AMoRe and automated package for molecular replacement. Acta Crystallogr. A *50*, 157–163.

Nicholls, A., Sharp, K.A., and Honig, B. (1991). Protein folding and association: insights from the interfacial and thermodynamic properties of hydrocarbons. Proteins *11*, 281–296.

Otwinowski, Z., and Minor, W. (1997). Processing of X-ray diffraction data collected in oscillation mode. Methods Enzymol. *276*, 307–326.

Renatus, M., Stennicke, H.R., Scott, F.L., Liddington, R.C., and Salvesen, G.S. (2001). Dimer formation drives the activation of the cell death protease caspase 9. Proc. Natl. Acad. Sci. USA *98*, 14250–14255.

Riedl, S.J., Fuentes-Prior, P., Renatus, M., Kairies, N., Krapp, S., Huber, R., Savesen, G.S., and Bode, W. (2001a). Structural basis for the activation of human procaspase-7. Proc. Natl. Acad. Sci. USA *98*, 14790–14795.

Riedl, S.J., Renatus, M., Schwarzenbacher, R., Zhou, Q., Sun, C., Fesik, S.W., Liddington, R.C., and Salvesen, G.S. (2001b). Structural basis for the inhibition of caspase-3 by XIAP. Cell *104*, 791–800.

Salvesen, G.S., and Duckett, C.S. (2002). IAP proteins: blocking the road to death's door. Nat. Rev. Mol. Cell Biol. *3*, 401–410.

Shi, Y. (2001). A structural view of mitochondria-mediated apoptosis. Nat. Struct. Biol. *8*, 394–401.

Shi, Y. (2002a). A conserved tetrapeptide motif: potentiating apoptosis through IAP-binding. Cell Death Differ. *9*, 93–95.

Shi, Y. (2002b). Mechanisms of caspase inhibition and activation during apoptosis. Mol. Cell *9*, 459–470.

Srinivasula, S.M., Saleh, A., Hedge, R., Datta, P., Shiozaki, E., Chai, J., Robbins, P.D., Fernandes-Alnemri, T., Shi, Y., and Alnemri, E.S. (2001). A conserved XIAP-interaction motif in caspase-9 and Smac/DIABLO mediates opposing effects on caspase activity and apoptosis. Nature *409*, 112–116.

Steller, H. (1995). Mechanisms and genes of cellular suicide. Science *267*, 1445–1449.

Sun, C., Cai, M., Meadows, R.P., Xu, N., Gunasekera, A.H., Herrmann, J., Wu, J.C., and Fesik, S.W. (2000). NMR structure and mutagenesis of the third BIR domain of the inhibitor of apoptosis protein XIAP. J. Biol. Chem. *275*, 33777–33781.

Terwilliger, T.C., and Berendzen, J. (1996). Correlated phasing of multiple isomorphous replacement data. Acta Crystallogr. D *52*, 749–757.

Thompson, C.B. (1995). Apoptosis in the pathogenesis and treatment of disease. Science *267*, 1456–1462.

Thornberry, N.A., and Lazebnik, Y. (1998). Caspases: enemies within. Science *281*, 1312–1316.

Verhagen, A.M., Ekert, P.G., Pakusch, M., Silke, J., Connolly, L.M., Reid, G.E., Moritz, R.L., Simpson, R.J., and Vaux, D.L. (2000). Identification of DIABLO, a mammalian protein that promotes apoptosis by binding to and antagonizing IAP proteins. Cell *102*, 43–53.

Wu, G., Chai, J., Suber, T.L., Wu, J.-W., Du, C., Wang, X., and Shi, Y. (2000). Structural basis of IAP recognition by Smac/DIABLO. Nature *408*, 1008–1012.

Yuan, J., and Yankner, B.A. (2000). Apoptosis in the nervous system. Nature *407*, 802–809.

Zou, H., Yang, R., Hao, J., Wang, J., Sun, C. Fesik, S.W., Wu, J.C., Tomaselli, K.J., and Armstrong, R.C. (2002). Regulation of the Apaf-1/caspase-9 apoptosome by caspase-3 and XIAP. J. Biol. Chem, in press. Published online December 27, 2002. 10.1074/jbc.M204783200.

Accession Numbers

The atomic coordinates for the caspase-9/BIR3 complex have been deposited with the Protein Data Bank under code 1NW9.